Receptor structure-based discovery of non-metabolite agonists for the succinate receptor GPR91

Trauelsen, Mette; Rexen Ulven, Elisabeth; Hjorth, Siv A; Brvar, Matjaz; Monaco, Claudia; Frimurer, Thomas M; Schwartz, Thue W

MOLECULAR
METABOLISM

Receptor structure-based discovery of non-metabolite agonists for the succinate receptor GPR91

Mette Trauelsen [1], Elisabeth Rexen Ulven [3], Siv A. Hjorth [2], Matjaz Brvar [3], Claudia Monaco [4], Thomas M. Frimurer [1],[*], Thue W. Schwartz [1],[2],[*]

ABSTRACT

Objective: Besides functioning as an intracellular metabolite, succinate acts as a stress-induced extracellular signal through activation of GPR91 (SUCNR1) for which we lack suitable pharmacological tools.

Methods and results: Here we first determined that the cis conformation of the succinate backbone is preferred and that certain backbone modifications are allowed for GPR91 activation. Through receptor modeling over the X-ray structure of the closely related P2Y1 receptor, we discovered that the binding pocket is partly occupied by a segment of an extracellular loop and that succinate therefore binds in a very different mode than generally believed. Importantly, an empty side-pocket is identified next to the succinate binding site. All this information formed the basis for a substructure-based search query, which, combined with molecular docking, was used in virtual screening of the ZINC database to pick two serial mini-libraries of a total of only 245 compounds from which sub-micromolar, selective GPR91 agonists of unique structures were identified. The best compounds were backbone-modified succinate analogs in which an amide-linked hydrophobic moiety docked into the side-pocket next to succinate as shown by both loss- and gain-of-function mutagenesis. These compounds displayed GPR91-dependent activity in altering cytokine expression in human M2 macrophages similar to succinate, and importantly were devoid of any effect on the major intracellular target, succinate dehydrogenase.

Conclusions: These novel, synthetic non-metabolite GPR91 agonists will be valuable both as pharmacological tools to delineate the GPR91-mediated functions of succinate and as leads for the development of GPR91-targeted drugs to potentially treat low grade metabolic inflammation and diabetic complications such as retinopathy and nephropathy.

1. INTRODUCTION

It is becoming increasingly clear that key metabolites function not only as energy sources and building blocks but can act also as extracellular messengers signaling through G protein coupled receptors (GPCRs) similarly to hormones and neurotransmitters [1]. Succinate, which has for many years solely has been viewed as a TCA cycle intermediate, is one of these signaling metabolites. Already in 2004, succinate was shown to be the ligand for the G-protein coupled receptor (GPCR) GPR91 [2]. The receptor was predominantly found to be expressed in the kidney, spleen, liver, and small intestine [2]. In the following years most attention was paid to the pro-hypertensive effect of GPR91 associated with renin-release [3]. In the liver, stress-induced succinate accumulation and GPR91 activation has been linked to development of fibrosis due to its expression in hepatic stellate cells, which, upon succinate stimulation, produces fibrogenic factors in a GPR91-dependent manner [4,5].

During normal physiological conditions, plasma levels of succinate range between 2 and 30 μM for humans and 6—17 μM for rodents [5—8]. These levels are below the reported EC50 values for GPR91 activation [1]; however, metabolic stress conditions such as hyperglycemia and hypoxia cause the levels of succinate to rise both locally and in the circulation, enabling activation of GPR91 [5,7,9—11]. Notably, several of the classical rodent models of metabolic dysfunction have all displayed elevated plasma levels of succinate [7], a finding also established in patients suffering from Type 2 diabetes (T2D) [12]. GPR91 has been proposed to be involved in the development of diabetes complications including neuronal VEGF-mediated neovascularization in diabetic retinopathy [3,13,14] as well as in diabetic nephropathy [9,15]. Adipocytes also express GPR91 and activation of the receptor inhibits lipolysis [16]. The physiological role of GPR91 on whole body metabolism, however, is still unclear as GPR91 deficiency in mice challenged with HFD has been reported both to give *impaired*

[1]NNF Center for Basic Metabolic Research, Section for Metabolic Receptology, Faculty of Health and Medical Sciences, University of Copenhagen, Blegdamsvej 3, 2200 Copenhagen, Denmark [2]Laboratory for Molecular Pharmacology, Department of Biomedical Research, Faculty of Health and Medical Sciences, University of Copenhagen, Blegdamsvej 3, 2200 Copenhagen, Denmark [3]Department of Physics, Chemistry and Pharmacy, University of Southern Denmark, Campusvej 55, 5230 Odense M, Denmark [4]Kennedy Institute of Rheumatology, University of Oxford, Roosevelt Drive, Headington, OX3 7FY Oxford, UK

*Corresponding authors. Novo Nordisk Foundation Center For Basic Metabolic Research, Blegdamsvej 3B, DK-2200 Copenhagen, Denmark. E-mails: thomas.frimurer@sund.ku.dk (T.M. Frimurer), tws@sund.ku.dk (T.W. Schwartz).

Original Article

[17] and *improved* glucose tolerance [12]. McCreath and colleagues also observed dramatic changes in WAT composition [17], something that also was not confirmed by van Diepen et al., who notably proposed that a dramatic decrease in infiltrating macrophages was the main driver of the improved glucose tolerance in GPR91 deficient mice [12]. In fact, GPR91 does seem to be an important regulator of innate immunity, particularly as an activator of dendritic cells [18] and macrophages [19].

Importantly, independent of GPR91 signaling, succinate can cause a number of intracellular responses, including post translational modifications [20], HIF-1α stabilization [21], production of mitochondrial reactive oxygen species (ROS) [11], and overall changes to cellular metabolism owing to its central role in the TCA cycle. Due to such non-receptor mediated effects, the endogenous metabolite succinate as such is not a reliable agent to delineate the specific physiological importance of GPR91. The aim of the present study, therefore, was to develop drug-like non-metabolite GPR91 agonists as potential pharmacological tools by use of a receptor structure-based approach.

2. MATERIALS AND METHODS

2.1. Compound acquisition and preparation

Ligands for library 1 and 2 were purchased from a range of vendors including Enamines, Vitas-M Laboratories, ChemDIv, Interbioscreen, and Key Organics. Succinate and other small carboxylic acids for Figure 1 were purchased from Sigma—Aldrich® and Akos.

All purchased compounds were spun down and subsequently dissolved in 100% dimethyl sulfoxide (DMSO) to achieve a final concentration of 50 mM and left to shake overnight. Dilution rows of the 50 mM stock solutions were subsequently prepared to obtain concentrations suitable for cell-based assays. It is important to mention that all presented structures were confirmed using proton (1H) NMR spectra at 300/400 MHz and liquid chromatography—mass spectrometry (LC-MS) analysis confirmed a minimum purity of 95% for all compounds.

2.2. Synthesis of enantiomerically pure compounds

All enantiomerically pure compounds were synthesized by the same general route. D- or ʟ-aspartate protected as the corresponding dimethyl esters were coupled with the appropriate carboxylic acid building block using fluoro-*N, N, N′, N′*-bis(tetramethylene)formamidinium hexafluorophosphate [22]. Lithium hydroxide-promoted ester hydrolysis gave the desired test compounds. The acid building blocks were either commercially available (compound 184), or synthesized by Williamson ether synthesis (compound 131) or by Suzuki cross coupling using Buchwald's fourth generation XPhos precatalyst [23] (compound 130), both followed by ester hydrolysis. Detailed procedures and compound characterization can be found in the Supplementary information.
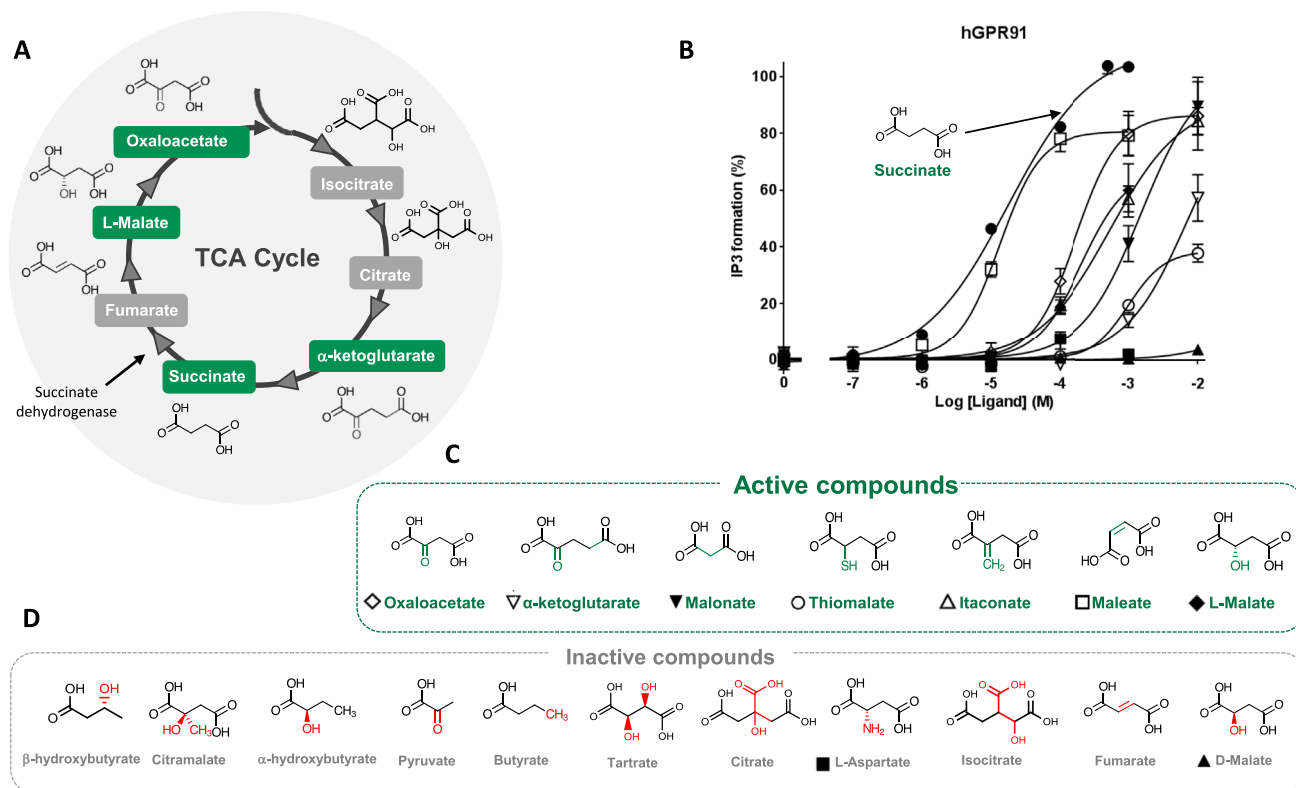

Figure 1: GPR91 activation properties of TCA cycle metabolites and synthetic succinate analogs. **A)** The main metabolites of the TCA cycle are depicted with structures. Compounds that are able to activate GPR91 are indicated in green and inactive compounds are in gray. **B)** Dose response curves for the 'active' succinate analogs measured as induction of IP3 turnover in GPR91 transfected HEK-293 cells (N = 3); L-aspartate and D-malate are included as representatives of the inactive compounds. Symbols used for each compound are annotated in panels C and D. **C)** Chemical structures of all compounds that were found to be able to activate GPR91. **D)** Chemical structures of compounds unable to activate GPR91. All compounds are named after their appearance at physiological pH; succinate instead of succinic acid, malate instead of malic acid etc. However, for esthetic reasons all compound structures are shown in their neutral form.

2.3. Homology modeling and molecular docking

Homology models of the human (UniProtID: Q9BXA5) and mouse (UniProtID: Q99MT6) GPR91 receptor was constructed using ICM 3.8 (Molsoft L.L.C. 11199 Sorrento Valley Road, S209 San Diego CA 92121) and the human P2Y1 receptor in complex with MRS2500 (pdbid: 4XNW) as a template (36% sequence identity, alignment shown in Figure S1). The models were relaxed using 300 steps of Cartesian minimization, followed by a global side-chain minimization (300 moves).

The initial homology models were further refined using Rosetta version 3.4 and subjected to 1,000 steps of full-atom structure relaxation using the membrane force field [24] using default parameters. The best scored model was converted into an ICM object and expanded by 21 models using elastic network modeling employing the ICM 3.8–5 (Molsoft L.L.C. 11199 Sorrento Valley Road, S209 San Diego CA 92121) to broadly sample the binding pocket geometry and the conformational variability of the receptor. 3D grid maps that represent the van der Waals, electrostatics, hydrophobic and hydrogen bonding potentials of the selected binding pocket residues were calculated using a grid spacing of 0.5 A and a margin of 4 A (default values) were generated sequentially for all receptor conformations in the stack. Against each of these models, we computationally docked succinate and the compounds in library 1 and 2 using the four-dimensional docking protocol (4D Docking) in ICM (using default parameter setting) [25]. The "docking effort" parameter controlling the number of Monte Carlo steps were set to 3. In brief, the scoring function uses steric, entropic, hydrogen bonding, hydrophobic and electrostatic terms to calculate the score and also includes a correction term proportional to the number of atoms in the ligand to avoid bias towards larger ligands [25].

2.4. Structure-based virtual screening of compounds

The *In-Stock* subset of ZINC (http://zinc.docking.org) containing 12,782,590 biologically relevant screening molecules stripped for counter ions and assigned stereomers, tautomers, protonation states, and charges were stored in fast search index files using Babel [26].

2.4.1. Library 1

A Markush substructure which included i) a carboxylic acid and/or acidic (bio)isostere ii) one — three atom linker to an acceptor and/or another carboxylic acid/acidic (bio)isoster and iii) up to three R groups connected to the linker atoms was used as a query to search the ZINC database. Several classes of accepted molecules were rejected based on the following criteria: compounds with long alkyl chains and many rotatable bonds, as well as compounds with high molecular weight (>450) and clogP (>5) were deprioritized. Accepted compounds were prioritized based on their predicted drug-like properties ($0.2 <$ drug-likeness score < 1.2) using the chemo-informatics tools in ICM 3.8 (Molsoft L.L.C. 11199 Sorrento Valley Road, S209 San Diego CA 92121). Compounds were furthermore prioritized between the commercial vendors based on their reliability and cost. Compounds that were structurally different from the succinate analogs (Figure 1) were preferentially chosen to maximize the number of different chemotypes. The remaining compounds were subsequent clustered using a T_c threshold = 0.3 and docked to the GPR91 model. A total of 111 compounds (Table S2) were purchased from two vendors based on manual assessment to recapitulate chemical complementary and key interactions of the GPR91-succinate model.

2.4.2. Library 2

The identified agonists 104 and 109 were used as seed structures for similarity-based searches of ZINC using FP2 fingerprints and a cut-off

Tanimoto Coefficient threshold, TC > 0.60. A total of 134 compounds (Table S3) were purchased from four vendors using the filter criteria above combined with SAR knowledge and predicted binding conformations of active library 1 compounds, which is a common accepted practice for cherry-picking compounds for experimental testing.

2.5. Molecular biology, cell culture, and transfection

The mGPR91 and hGPR91 receptor constructs were obtained from Origene and cloned into the eukaryotic expression vector pCMV-Tag (2B) (Stratagene). Point mutations were introduced by PCR using the QuickChange method. All PCR reactions were performed using *Pfu* polymerase (Stratagene) according to manufacturer's instructions. DNA was purified from transformed cells carrying one specific point mutation with midi prep kit from Qiagen. All constructs were verified by DNA sequence analysis by GATC Biotech (GATC) (Constance, Germany).

HEK-293 cells were grown in Dulbecco's modified Eagle's medium 1885 (DMEM) supplemented with 10% fetal calf serum, 100 units/ml penicillin, and 100 μg/ml streptomycin. HEK-293 cells were transiently transfected with Lipofectamine-2000 according to manufacturer's protocol and supplemented with fresh medium after 5 h.

2.6. IP3 turnover assay

HEK-293 cells were plated in poly-D-lysine-coated 96-well plates (35.000 cells/well). The following day, cells were transfected in 100 μl transfection medium/well for a total of 5 h and thereafter incubated with 0.5 μCi/ml myo [^{3}H]inositol (Perkin Elmer) in 100 μl growth medium O/N. The subsequent day cells were washed twice with 200 μl/well HBSS (Gibco, Life Technologies) and pre-incubated for 30 min at 37 °C with 100 μl buffer supplemented with 10 mM LiCl. Ligand addition was followed by 120 min incubation at 37 °C. Cells were lysed with 50 μl 10 mM formic acid followed by incubation on ice for 30 min, 20 μl of the extract was transferred to a white 96-well plate and 80 μl of 1:8 diluted YSi SPA scintillation beads (Perkin Elmer) was added. After vigorous shaking, the plate was centrifuged for 5 min at 1500 rpm, and light emission (scintillation) was recorded on a Packard Top Count NXT counter after an 8 h delay. Determinations were made in triplicates.

2.7. Ca^{2+} mobilization assay

40.000 HEK-293 cells/well were plated in poly-D-lysine-coated black, clear bottom 96-well plates (Corning®). The following day, the cells were transfected with either mGPR91, hGPR91, or empty vector control for 5 h in 100 μl transfection medium/well and thereafter supplemented with full medium O/N. The following day cells were incubated at 37 °C in 50 μl loading buffer/well (wash buffer: HBSS (Gibco, Life Technologies) supplemented with 1 mM CaCl$_2$, 1 mM MgCl$_2$, 2.5 mM Probenicid supplemented with 0.2% Fluo-4). After 1 h cells were washed twice with wash buffer and 100 μl wash buffer was added/well for the assay. Cells and compounds were transferred to the Flexstation 3 (Molecular devices, USA) and Fluo-4 fluorescent signals (relative fluorescence unit, RFU) were recorded. Settings: 90 μl height, 76 measurings, injection rate, injection vol. 25 μl. Data were baseline corrected and presented as dose-response curves of Max RFU — Min. RFU.

2.8. SDH assay

Succinate dehydrogenase activity was measured by a colorimetric assay kit from Biovision (Cat# K660-100) and performed according to manufacturer's instructions. In brief, 6 million HEK-293 cells/well were

harvested and washed in 1 ml PBS. The cells were then centrifuged and resuspended in 600 μl SDH buffer and centrifuged again for 10 min, 4 °C. Supernatant was transferred to a new eppendorf tube and kept on ice. Supernatant was added to a 96 well plate, and compounds and inhibitors were added to each well and pre-incubated for 5 min. Standard and positive controls were then loaded and reaction mix added to each well. Absorbance was measured at 595 nm and activity calculated as advised by the manufacturer.

2.9. Macrophage isolation, culture and stimulation

Human monocytes were separated and purified by centrifugal elutriation. Briefly, human PBMCs were obtained by density centrifugation through Ficoll of a single-donor platelet depleted residue (North London Blood Transfusion Service, Colindale, UK). The resulting PBMCs were centrifugally elutriated in 1% heat-inactivated FBS in RPMI in a Beckman JE6 elutriator (Beckman, High Wycombe, UK). Monocytes separated by this method were assessed for purity by flow cytometry (FACSCan, Becton Dickinson, Oxford, UK) and were greater than 80%. The purified monocytes were stimulated with MCSF (100 ng/ml) in 10 cm dishes in RPMI + 10% FCS at a density of 1×10^6 cells/ml for 5 days at 37 °C (5% CO_2). On day 5 the MCSF differentiated cells were lifted, counted, and re-stimulated for 24 h with IL-4 + IL-13 (20 ng/ml) in 24 well plates at a density of 1×10^6 cells/ml at 37 °C, 5% CO_2. On day 6, the medium was removed and cells were stimulated with either DMSO (final conc. 0.1%), succinate (100 μM and 500 μM), or compound 131 (10 μM and 100 μM). Cells were harvested after 2 h and 24 h incubation at 37 °C (5% CO_2), washed twice with PBS, snap frozen in liquid nitrogen, and stored at −80 °C until RNA extraction was performed.

2.10. RNA extraction and gene expression

RNA from 1 mio. macrophages/condition was extracted using the Nucleospin RNA kit (Macherey–Nagel) according to manufacturer's instructions. In brief, cells were lysed with Buffer RA1 and β-mercaptoethanol for 2 min in a TissueLyser LT (Qiagen). Samples were filtered on NucleoSpin Filter columns, and RNA was captured on NucleoSpin RNA columns. Samples were DNase treated for 15 min and eluted in 40 μl RNase free H_2O. RNA concentration and quality was measured on NanoDrop 2000 (Thermo Scientific™).

cDNA was made using the Invitrogen SuperScript® III First-Strand synthesis system for RT-PCR according to manufacturer's instructions. In brief, RNA concentrations were adjusted to equal values and two consecutive RT reactions were made. RT1 mastermix consisting of 5× FS buffer, random primers, and 0.1M DTT was added to each concentration-adjusted RNA sample. Samples were heated to 70 °C for 3 min. RT2 was then performed by adding mastermix (dNTPs, RNaseOUT, Superscript III) to each sample and running a PCR program of 5 min at 25 °C, 60 min at 50 °C, and 15 min at 70 °C. cDNA was stored at −20 °C.

qPCR was performed in duplicates in 384 well plates; cDNA was diluted 20-fold and mixed with PrecisionPLUS MasterMix premixed with SYBRgreen (Primerdesign®). All samples were run on a Lightcycler 480 ll (Roche) using the program: 1 cycle of 2 min 95 °C, 45 cycles of 15 s 95 °C, 1 min 60 °C. CT values were calculated by the 2nd derivatives method and expression was evaluated by the ΔΔCT method [27], normalizing expression to GAPDH expression. Data are presented as fold change and primer sequences can be found in the Supplementary section Figure S2.

2.11. Statistical analysis

Data are presented as mean ± standard error of the mean (SEM) of absolute values, % changes or fold changes as indicated in the figures. Data were analyzed using a one-way ANOVA multiple comparisons test (GraphPad Prism). Statistical tests used are mentioned in the figure legends. Values were regarded as significant when $P < 0.05$.

3. RESULTS

3.1. Structure-activity relationship (SAR) for succinate activation of GPR91

To obtain information about the SAR for succinate binding and activation of GPR91, we tested a small library of 18 succinate analogs including other TCA cycle metabolites in transiently transfected HEK293 cells overexpressing human GPR91 plus the modified, promiscuous G protein Gqi4myr. Gqi4myr allows the otherwise presumably Gi coupled GPR91 to give a robust signal through Gq measuring in this case IP3 accumulation (Figure S3) [28]. In this assay, succinate activated hGPR91 in a dose-dependent manner (EC50 = 17 μM) (Figure 1B). Interestingly, three of the other TCA cycle metabolites could also activate GPR91 albeit with lower potencies than succinate: oxaloacetate (EC50 = 171 μM), L-malate (EC50 = 207 μM) and α-ketoglutarate (EC50 = 7.3 mM) (Figure 1B). As shown in Figure 1B and c, we also found four other dicarboxylic acid metabolites to be agonists for GPR91 with maleate (a known GPR91 agonist) being equally potent (EC50 = 13 μM) and almost equally efficacious as succinate, whereas itaconate and malonate both had potencies around 1 mM (Figure 1B). Although the physiological importance of these non-succinate metabolites as ligands for GPR91 is doubtful, the fact that the metabolites shown in Figure 1C are agonists for GPR91, in contrast to a number of other very similar metabolites and synthetic compounds shown in Figure 1D, provides important information about the structural requirements for binding and activation of this receptor by small dicarboxylic acid compounds. For example, the high potency and efficacy of maleate, in contrast to the stereoisomer fumarate, indicates that the cis backbone conformation is optimal (Figure 1). Similarly, it is clear that certain, but not other, modifications of the succinate backbone are allowed, for example -OH versus -NH2 (L-malate versus L-aspartate) and that the stereochemistry of the backbone substitution has to be in the L-configuration (L-malate versus D-malate).

No IP3 response was observed with any of the active compounds in cells transfected only with the promiscuous G protein. However, as several of the compounds including malonate, itaconate, and oxaloacetate are known to inhibit succinate dehydrogenase (SDH), which could lead to accumulation of succinate and subsequent indirect activation of GPR91, we further validated our findings in Ca^{2+} signaling assays, which, in contrast to the IP3 assay, provide a very quick response (i.e. within ∼2 s). All compounds gave clear, rapid increases in intracellular calcium (Figure S4), indicating that these compounds most likely act directly as agonists on GPR91.

In agreement with a recent report from Geubelle and coworkers [29], the main conclusion from the initial SAR analysis using succinate analogs was that the cis conformation of the backbone is preferred and that certain substitutions of the succinate backbone are allowed, thus encouraging further search for non-metabolite GPR91 agonists.

3.2. GPR91 receptor modeling and molecular recognition of succinate

From an evolutionary point of view, GPR91 is closely related to the purinergic receptors (Figure 2A) and in particular P2Y1 for which a high resolution X-ray structure was recently published [30]. Using a combination of ICM (Molsoft L.L.C. 11199 Sorrento Valley Road, S209 San Diego CA 92121) and the Rosetta modeling package, which sample backbone and loop conformations by fragment assembly, we

generated a three-dimensional hGPR91 homology model, using the structure of hP2Y1 as a template. Based on molecular modeling and mutagenesis, it was originally proposed that succinate in GPR91 would bind between three arginine residues, Arg[99] (ArgIII:05/3.29), Arg[252] (ArgVI:20/6.55) and Arg[281] (ArgVII:06/7.39) located in the pocket between the extracellular segments of TM-III, -VI and -VII [2]. Importantly in P2Y1, the guanidino functions of ArgIII:05 and ArgVI:20, from each side interact closely with Asp[174], which points deep into the main ligand binding pocket from ECL-2b, the backbone of which forms an unusual loop buried in the pocket (Figure 2B). This complex is apparently further stabilized by a number of interactions with other highly conserved polar residues: His[103] (HisIII:09), Tyr[277] (TyrVII:02) and Arg[281] (ArgVII:06). All of the indicated residues are conserved in GPR91 relative to the purinergic receptors and in the model of GPR91 these residues form a similar, apparently very stable complex filling the deep part of the main ligand binding pocket. Based on this observation, we reasoned that Arg[99] (ArgIII:05) and Arg[252] (ArgVI:20) are probably not directly involved in succinate binding, despite the fact that we could confirm the original observation that mutational substitution of these two residues severely impaired succinate activation of GPR91 (Table S1). Conceivably, these effects are indirect and likely related to disruption of the special 'plug' structure of ECL-2b in part of the main ligand binding pocket. Interestingly, the [R95L]mGPR91 receptor construct displayed very high constitutive activity not observed in the wildtype receptor (Figure 2D).

As the basis for in silico screening, the top scored GPR91 models were expanded to another 21 models through elastic network modeling using ICM v.3.8 (Molsoft L.L.C., San Diego, CA, USA) to broadly sample the binding pocket geometry and the conformational variability of the receptor. Against each of the 21 models, we computationally docked succinate using an ensemble docking strategy called four-dimensional docking (4D Dcoking) in ICM [25], which effectively consider all structures in the ensemble in a single docking run. Investigation of the top ranked binding conformations revealed that the central CH_2-CH_2 of the succinate backbone functions as a spacer for optimal positioning of the two terminal carboxylic acid moieties to make salt—bridge interactions with the originally proposed 'third' arginine residue, Arg[281] (ArgVII:06) and a previously unnoticed Arg[255] (ArgVI:23) located one helical turn above Arg[252] (ArgVI:20) in TM-VI and interestingly also picking up interactions with the backbone -NH of Asp[174] (Figure 2E). The strongly impaired potency of succinate upon mutational substitution of Arg[255] (ArgVI:23) supported the notion that this is involved in ligand binding (Figure 2D). The proposed binding conformation of succinate is in agreement with the structure activity relationship of the succinate analogs (Figure 1), i.e. in particular the activity of maleate vs. fumarate indicating a preferred cis conformation of the backbone in the binding pose (Figure 2E).

Thus, the P2Y1 receptor based molecular modeling and docking identified what we believe is the real binding site for succinate in GPR91 and, importantly, the model of the succinate-GPR91 complex reveals
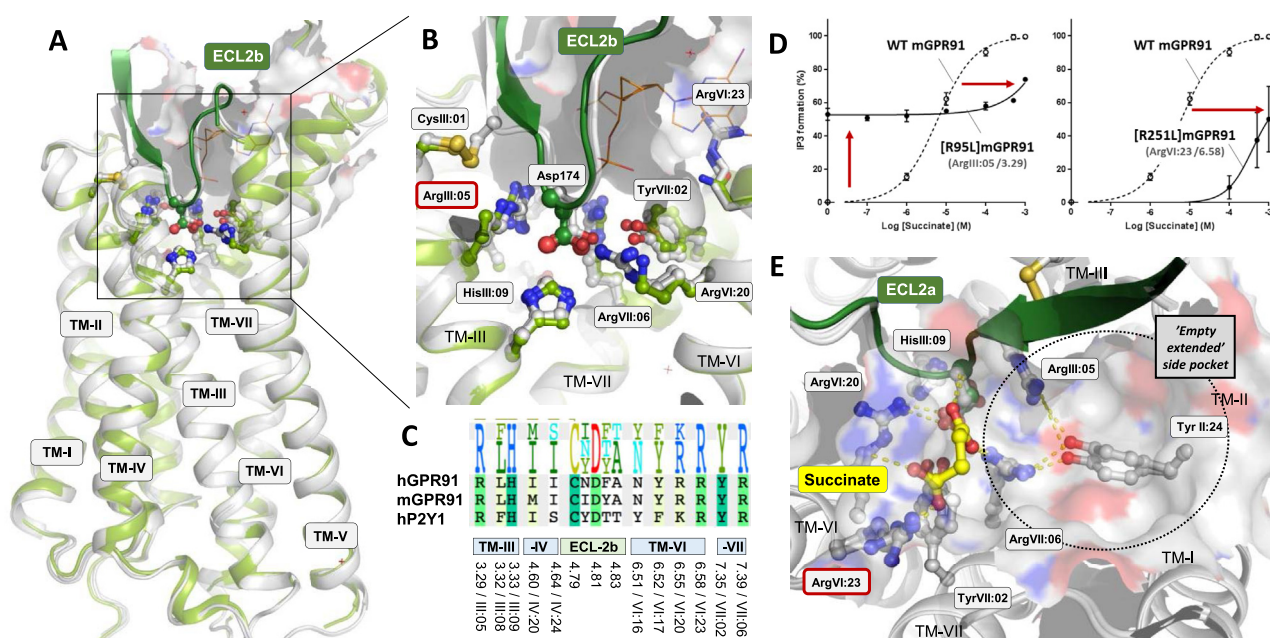

Figure 2: Molecular modeling of the GPR91-succinate complex. A) Comparison of the of P2Y1 X-ray structure (pdbid:4xnw, green) and the homology of the human and mouse GPR91 receptors (gray) generated based on the P2Y1 structure with ECL-2b buried deep in between TM-III, -V and −VI highlighted in dark green. Side view from TM-IV and −V. **B)** Detailed side view (with TM-IV and −V removed) of the interactions between ECL-2b — in particular Asp174 — and transmembrane residues in the P2Y1 receptor and the corresponding interactions in the models of hGPR91 and mGPR91. **C)** 'Pseudo-sequence' of conserved network of polar and positively charged residues, which are found close to Asp174 (ECL-2b) in the main ligand binding pocket of P2Y1, and h and mGPR91. Positions are annotated both with Ballesteros Weinstein and Schwartz numbering (used in most figures). **D)** Dose-response curves for succinate in HEK-293 cells transfected with either the WT mGPR91 (dotted line) or the [R95L]mGPR91 (Arg:05/3.29) (left panel) proposed to affect activity as shown in panel B or [R251L]mGPR91 (ArgVI:23/6.58) (right panel) which is proposed to affect activity directly through interaction with succinate binding panel E. Red arrows indicate shifts in potency and efficacy induced by mutations (N = 3). **E)** Extracellular view of the top-ranking binding conformation of succinate (yellow) in complex with hGPR91. Note interaction of one caboxylate of succinate with the backbone -NH of Asp174 in ECL-2b and with ArgVII:06 (from the 'bottom' of the pocket) and the other carboxylate with ArgVI:23. The unoccupied pocket extending towards TM-I and −II from the proposed binding site of succinate, which we in the following try to exploit for binding of synthetic succinate analogs is indicated by a dotted circle.

that a relatively large empty pocket extends towards TM-I and —II from this binding site of succinate; i.e. a pocket which potentially could be exploited by succinate analogs for binding (Figure 2E).

3.3. Identification of non-metabolite GPR91 agonists

Computational screening of the ∼ 12 million compounds of the in-stock subset of the ZINC database [31] was performed using a combination of large scale substructure searches and molecular docking (see methods for details). The search query was based on a Markush substructure which included i) a carboxylic acid and/or acidic (bio)isosters corresponding to one of the two carboxylates of succinate; ii) a one to three atom linker to an acceptor and/or another carboxylic acid/acidic (bio) isoster corresponding to the other COOH of succinate; and iii) up to three R groups connected to the linker atoms, supported by the GPR91-succinate models (Figure 3A). The positive hits were filtered based on drug-like properties and cluster analysis of 652 accepted compounds revealed 139 cluster representatives using a Tc threshold of 0.3. A small library of 111 compounds was selected and acquired based on subjective investigator (TMF) inspection and assessment of chemical complementary and key interactions of the GPR91-succinate model (Table S2). The 111 compounds were tested for their ability to activate GPR91 expressed in transfected HEK293 cells. Twenty compounds from library #1 displayed potencies below 1 mM on the human and mouse GPR91 and two compounds (compounds 48 and 104) were almost as potent as succinate on the human receptor (Figure 3B). Dose-response curves and structures for the three hits with the highest potency on human GPR91 are shown in Figure 3C. Compound 48, 1,2-cyclopropane-dicarboxylic acid, has recently been identified as a GPR91 agonist among succinate analogs [29]. Molecular docking of compound 104 demonstrated that the left hand-side succinate moiety docked in a similar mode as succinate itself while the amide-linked hydrophobic right hand-side docked into the extended side pocket (Figure 3D). Due to the limited availability of extended analogs of compound 48, we chose to focus on compounds 104 and 109, which were used as seed structures for substructure and similarity-based searches including structural knowledge of SAR and predicted binding conformations to acquire a second-generation library (library #2, Table S3) containing 134 compounds. Only 12 compounds — most of which were analogs of compound 104 — displayed potencies below 1 mM on both the human and mouse GPR91 receptor (Figure 4A). Non-amide linked analogs of compound 104 were all negative, explaining the relatively low hit rate in library #2. However, among the amide linked
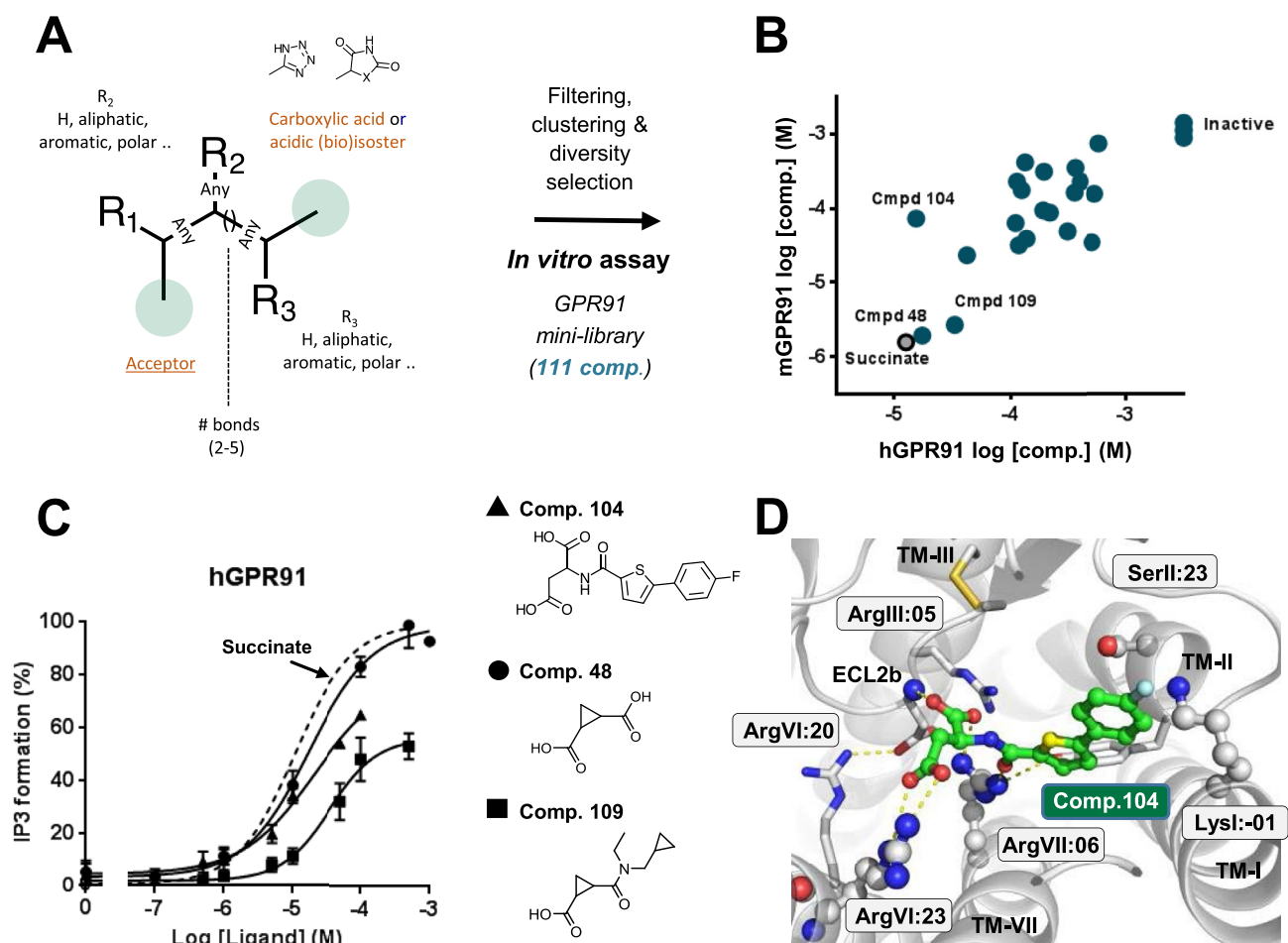

Figure 3: **Generation of initial succinate-based GPR91-targeted compound library**. **A)** Schematic illustration of the multivariable Markush structure used for virtual screening of the ZINC database containing >12 million biologically relevant compounds. **B)** Scatterplot of agonist potencies of the 111 compounds of library #1 tested by IP3 accumulation in GPR91 transfected HEK-293 cells. **C)** Dose response curves and structures of the three most potent hits from library #1 on human GPR91: comp. 48, 104 and 109. **D)** Compound 104 (in green) docked into the molecular model of hGPR91 (gray). Yellow dashed line indicated proposed hydrogen bonds.
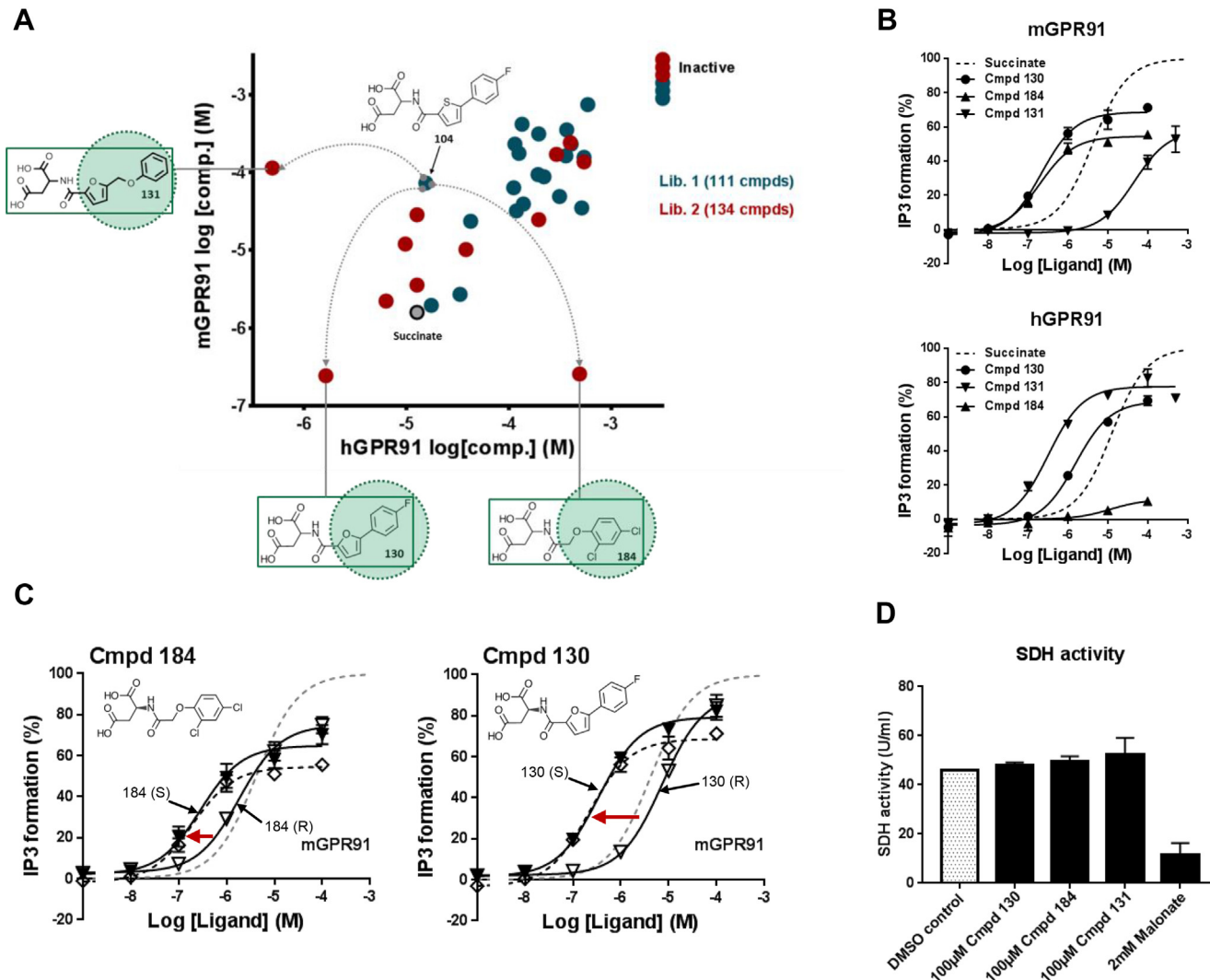
Figure 4: Generation of second GPR91-targeted library based on compounds 109 and 104 from library #1 including stereochemical clarification and SDH activity of the most potent compounds. A) Scatterplot of *in vitro* agonist potencies of library #1 (blue circles) and #2 (red circles) on the human and mouse GPR91 receptor, including chemical structures of the most potent hits, as determined from IP3 accumulation assays in transfected HEK293 cells. B) Dose response curves of comp. 130, 131, and 184 on mGPR91 (top) and hGPR91 (bottom) (N = 3) as compared to succinate (dotted line). C) The effect on IP3 turnover for the racemate of comp. 184 (left panel) and comp. 130 (right panel) (black dotted lines) and the (S) and (R) enantiomers of each of these compounds as indicated, compared to succinate (gray dotted line). All compounds are tested on mGPR91 (N = 3). D) Succinate dehydrogenase (SDH) activity during stimulation with comp. 130, 184, and 131 (100 μM), and malonate (2 mM) included as a positive inhibitory control (N=2).

analogs, eight compounds displayed up to 50-fold improved potency on the human and up to 200-fold improved potency on the mouse GPR91 receptor (Figure 4A). Among these, compound 131 was highly selective for the human receptor, compound 184 was highly selective for the mouse receptor, and compound 130 displayed high potency for both (EC50 on hGPR91 = 1.9 μM and EC50 on mGPR91 = 215 nM), with compounds 130 and 131 both having more than 10-fold higher potency than succinate on hGPR91 (Figure 4B). The structural basis for the species selectivity of the compounds is likely related to one or more of the six amino acid residues, which differ between the mouse and the human receptor in the proximity to the 'side-pocket' where the amide-linked hydrophobic moiety of these compounds bind (Table S1). All three compounds appeared to be 60—80% partial agonists as compared to succinate in the IP3 signaling assay.

As the positive synthetic non-metabolite compounds all have a stereo center around the succinate backbone carbon where the amide linker is attached, we synthesized the R and S form of each compound and tested them for GPR91 activation. As observed for the metabolite succinate analogs, the S-form of all three compounds was more potent than the R-form; 21-fold for compound 130 and 6.4-fold for compound 184 (Figure 4C), and 6.7-fold for compound 131 (not shown). That the differences between the two stereoisomers were not larger could be related to the possibility for multiple different interaction modes of the succinate moiety (see below).

The starting point of this study was that the novel synthetic GPR91 agonists should be selectively acting as receptor ligands and not as intracellular metabolites. We therefore tested whether the compounds affected succinate dehydrogenase (SDH) activity, which is the case for

1591

a number of metabolite succinate analogs. As shown in Figure 4D, in contrast to the positive control malonate, none of the GPR91 positive synthetic compounds affected SDH activity.

3.4. Chemical novelty and selectivity of the non-metabolite GPR91 agonists

To assess the novelty of compounds 130, 131, and 184, we compared their two dimensional structural similarities to ~1.5 million annotated chemicals in the ChEMBL20 database [32]. The similarity was quantified by computed Tanimoto coefficients (Tc) based on 2D fingerprints using Babel [26]. The highest Tc to compounds in ChEMBL was 0.75, 0.85, and 1.0 for compounds 130, 131, and 184, respectively. Since the maximal Tc values of 1.0 is obtained for identical compounds, whereas smaller values represent lower similarity, compounds 130 and 131 represent truly novel chemotypes as they are chemically distinct from compounds previously reported to be active on other protein targets (Table S4). Importantly, despite the fact that compound 184 has been used in general screens, it is not reported to possess significant activities on any targets [32].

We furthermore subjected compound 130 to a screen in both agonist and antagonist mode on the 165 non-GPR91 GPCR receptors (gpcrMAX) in the DiscoverX profiling service (https://www.discoverx.com), and no significant activity (all < 30%) on any of the targets was observed (data not shown).

3.5. Docking and mutational analysis of non-metabolites versus succinate in GPR91

Compounds 130 and 131 were probed in the human and compounds 130 and 184 in the murine GPR91 receptor (Table S1). As shown in Figure 5A and E, both compound 131 and compound 184 docked nicely into the main ligand binding pocket of the receptor with the succinate moiety interacting with the central arginine residues and with the amide-linked hydrophobic groups located in the extended side pocket reaching over to TM-I and −II. Interestingly, the preferred binding pose for the succinate moiety of the non-metabolite compounds was slightly different from that of succinate itself. Although a cis conformation of the backbone was preferred, and each of the two carboxylic acid moieties interacted closely with ArgVII:06 and ArgVI:23, no interaction with the backbone -NH group of Asp[174] of ECL-2b was observed in contrast to the unmodified succinate. Instead in both compounds the carboxylate moiety next to the amide-linker apparently picked up interactions with the guanidino function of ArgIII:05, which was not observed with the unmodified succinate (Figure 2E vs. Figure 5A and E). Importantly, a close H-bond interaction of the amide linker with the guanidino moiety of ArgVII:06 was observed, which would explain the strong dependency of the amide linker in analogs of compound 104 in library #2 and the somewhat different pose of the neighboring succinate moiety of these compounds as compared to the unmodified succinate.

The mutational analysis demonstrated that the activity of all three compounds was totally dependent upon ArgVII:06 as observed also for the unmodified succinate (Figure 5B and F) and was also severely impaired by substitution of ArgVI:23 similar to succinate (Figure 5G). Among the effect of the other mutations in the binding pocket, the most important and differentiating ones were those involving substitutions at the extracellular ends of TM-I and II (Table S1). Thus, while the Phe-substitution of the Lys residue just preceding TM-I (LysI:-01) slightly improved the potency of both compounds 130 and 131 (Figure 5C),
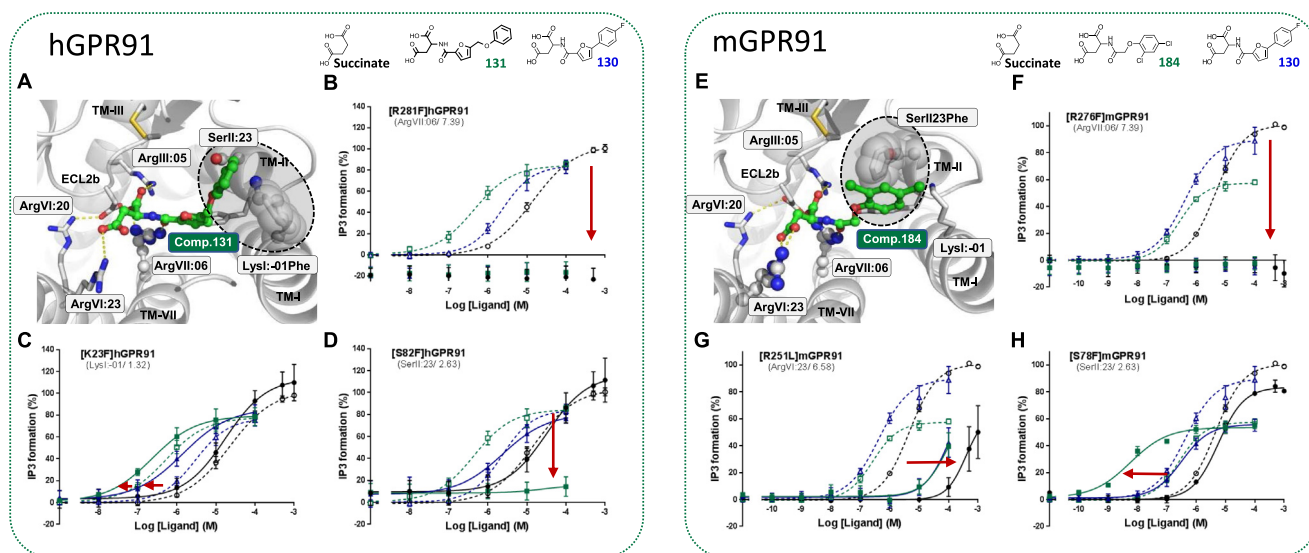

Figure 5: Mutational mapping of novel synthetic non-metabolite GPR91 agonists exploiting the side-pocket to the succinate binding site in GPR91. A) Molecular model of hGPR91 in complex with the human selective comp. 131 (green) with the succinate moiety binding with one carboxylate interacting with ArgVI:23 and the other carboxylate with ArgIII:05 and ArgVII:06 which also binds the amide linker. To the right are highlighted the proposed edge to face aromatic interaction between the terminal aryl of comp. 131 and the phenylalanine introduced in the gain-of-function mutation [K23F]hGPR91 (LysI:-01/1.32) (gray transparent spheres). Dose response curves for succinate (black) comp. 131 (green), and comp. 130 (blue) in selected mutant forms of human GPR91 are show in: B) [R281F]hGPR91 (ArgVII:06/7.39), C) [K23F]hGPR91 (LysI:-01/1.32), and D) [S82F]hGPR91 (SerII:23/2.63) in all panels compared to WT hGPR91 in dotted lines. Chemical structures of all compounds are shown at the top. E) Molecular model of mGPR91 in complex with the murine selective comp. 184 (green) with the succinate moiety binding with one carboxylate interacting with ArgVI:23 and the other carboxylate with ArgIII:05 and ArgVII:06 which also binds the amide linker in a similar manner as comp. 131 in the human receptor (panel a). Dose response curves for succinate (black) comp. 184 (green), and comp. 130 (blue) in selected mutant forms of murine GPR91 are shown in: F) [R276F]mGPR91 (ArgVII:06/7.39), G) [R251L]mGPR91 (ArgVI:23/6.58), and H) [S78F]mGPR91 (SerII:23/2.63). Chemical structures are shown at the top. Red arrows indicate shifts in potency and efficacy induced by mutations.

conceivably through establishing an aromatic—aromatic interaction with the terminal phenyl moiety of these compounds (Figure 5A), this substitution had no effect on succinate. Most significantly, Phe-substitution of SerII:23 at the extracellular end of TM-II in mGPR91 strongly improved the potency of compound 184 (from EC50 = 267 nM to 6 nM) (Figure 5H) likely through establishment of an edge-to-face aromatic—aromatic interaction with the terminal aryl group (Figure 5E). The similar SerII:23 to Phe substitution did not affect compound 130 neither in mGPR91 nor in hGPR91, but it totally eliminated the activity of compound 131 conceivably through steric hindrance as compound 131 is longer than compound 130 (Figure 5D). As expected, the [SerII:23Phe] substitution had no effect on succinate in agreement with its presumed binding site far away from TM-II.

It is concluded that the synthetic succinate analogs bind in the main ligand binding pocket of GPR91 with the succinate moiety mimicking the binding mode of unmodified succinate with minor yet significant differences caused by the interaction of not only one of the carboxylates, but importantly also the carbonyl of the amide linker as a main anchor point interacting with ArgVII:06. The hydrophobic moieties of these compounds dock into the extended side pocket to reach over to residues at the extracellular end of TM-I and —II, which is substantiated through both loss-of-function but also major gain-of-function mutagenesis.

3.6. Comparing *ex vivo* effect of non-metabolite compounds with succinate

Above we have only studied effects of the synthetic non-metabolite compounds on a single signal transduction pathway and in transfected HEK293 cells. In order to probe the effects of these compounds on biological endpoints in cells endogenously expressing GPR91, we turned to macrophages, which are known to express GPR91 [12,18,19]. However, as shown in Figure 6A, we find that GPR91 is particularly highly expressed in 'alternatively activated' macrophages (often referred to as M2 macrophages) generated from primary cultures of human monocytes by a combination of IL-4 and IL-13 as opposed to 'classically activated macrophages' (often referred to as M1 macrophages) i.e. stimulated by interferon-γ (IFNγ) and LPS. Consequently, we studied the effects of compound 131 on cytokine expression in primary cultures of human alternatively activated macrophages and compared it with succinate. Both compound 131 and succinate suppressed the expression of IL-10 and apparently increased the expression of TNF-α in the alternatively activated macrophages in a rather similar manner (Figure 6B). Compound 131 and succinate also suppressed the expression of toll like receptors (TLR) 4 and 5 in a similar manner.

It is concluded that the novel synthetic non-metabolite GPR91 agonists act as potent and efficacious GPR91-dependent agonists affecting human macrophage function in a similar manner as succinate, indicating that these effects of succinate are mediated via GPR91 and not via its effects as a classical metabolite.

4. DISCUSSION

In the present study, we describe the structure-based discovery of high potency, synthetic, non-metabolite partial agonists for the succinate receptor GPR91. The best compounds were backbone modified analogs of succinate, in which an amide-linked hydrophobic moiety fitted into an extended side pocket next to the succinate binding site. The compounds, which displayed similar GPR91 dependent activities in human macrophages as succinate, for example, but did not affect the major intracellular succinate target SDH, were discovered through generation of GPR91-customized mini-libraries picked through virtual screening of commercially available compounds.

4.1. Site-directed discovery of novel non-metabolite agonists for GPR91

We originally developed this basic technology in the biotech industry to obtain hits and leads in GPCR drug discovery [33]. Here we have applied the technology in a modified form in an academic setting, and successfully identified nanomolar agonists for GPR91 through the generation of two mini libraries of less than 250 compounds in total — while employing the synthesis of only a few novel compounds to solve the stereochemistry of receptor recognition. Recently we have applied the original site-directed approach to the Zn^{2+} sensor GPR39 by using its endogenous ligand Zn^{2+} [34—36] as an essential allosteric modulator to bring low-potency hits into the working range of the biological assays [37]. In the case of GPR91, our initial SAR analysis indicated that certain back-bone modifications of succinate were allowed and that the cis conformation of the backbone was preferred. Furthermore, our molecular modeling and computational chemistry analysis demonstrated that an empty pocket was located next to the succinate binding site. These observations were important for the design of our multivariable substructure-based search query for the virtual screening, which we believe was key to the success of the approach and the limited size of the mini-libraries.

In the academic setting, the present cost-efficient computational approach complements "random" experimental testing of large compound collections, e.g. High-Throughput Screening (HTS) which currently is becoming available in a number of institutions [38]. A major advantage of the computational approach is that it allows for bias in the
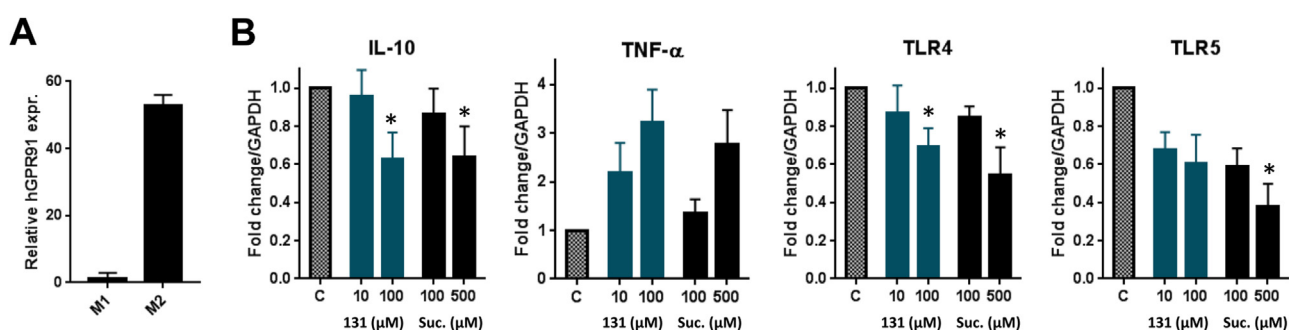

Figure 6: Effects of synthetic, non-metabolite GPR91 agonists and succinate on human macrophage gene expression. A) Expression of hGPR91 in human M1 and M2 macrophages determined by qPCR (N = 3). **B)** Effect of succinate (black columns) and compound 131 (dark blue columns) on the expression of IL-10, TNF-α, TLR4 and TLR5 in M2 macrophages determined by qPCR (N = 3). * P < 0.05, one-way ANOVA multiple comparisons test.

search strategy toward specific aims, such as e.g. enhancing certain physiochemical and/or pharmacological properties of particular novel chemotypes, and importantly, requiring only limited chemical synthesis. Application of other types of structure-based virtual screening approaches, using the actual ligand-binding sites of high-resolution X-ray structures of GPCR-ligand complexes, have proven to be similarly efficient in identifying novel ligands for these sites [39—44].

Recently the Roth and Shoichet groups have with great success applied such docking approaches to opioid and opioid-like receptors. Through computational docking of more than 3×10^6 compounds they identified new scaffolds for the μ-opioid receptor and eventually identified a novel agonist with minimal activation of the arrestin signaling pathway and associated respiratory depressive side effects [45]. Similarly, for the atypical opioid receptor MRGPRX2, a novel potent and selective agonist was identified through screening of 5.500 compounds and subsequent docking of nearly 4×10^6 compounds into the receptor based on the initially identified hits [46]. Such studies, together with the present study, illustrate the potential of applying computational chemistry based technologies and receptor structures or models for the identification of novel pharmacological tool compounds and potential drug leads in the academic setting.

4.2. Elucidation of the presumed binding site for succinate in GPR91

Mutagenesis has for many years been used extensively for identification of ligand binding sites in GPCRs [47]. However, it is very difficult to differentiate between direct and indirect effects of mutations. In the case of GPR91, it was originally proposed based on receptor mutagenesis that succinate would bind between three arginine residues located in what generally was considered to be the main ligand binding pocket of GPCRs [2]. This binding site was recently 'confirmed' by another group [29]. However, our molecular modeling of GPR91 over the recently published high resolution X-ray structure of the closely related P2Y1 purinergic receptor revealed that two of the three originally identified arginine residues (ArgIII:05/3.29 and ArgVI:20/6.55), which were believed to interact directly with succinate, are in fact both bound up in interactions with an aspartate residue, Asp^{174}, located in an extracellular loop (ECL-2b), which makes an unusual loop down into the main ligand binding pocket. These residues and the special loop of ECL-2b are conserved among the purinergic receptors to which GPR91 structurally belongs [30]. This knowledge enabled us to identify what we believe is the real binding site for succinate located between the 'third' originally identified ArgVII:06/7.39 and the previously unnoticed ArgVI:23/6.58. This binding site was used as part of the basis for the search query in the virtual screening of compounds (see above). We believe that the deleterious effects of mutational substitutions of the 'two other' arginine residues, ArgIII:05 and ArgVI:20 [2,29], i.e. effects which we could confirm, are indirect and caused by major changes in the structure of the whole binding pocket due to destabilization of the complex which holds part of ECL-2b down in the pocket. Interestingly, we observed that mutational substitution of ArgIII:05 in GPR91 resulted in a very high constitutive signaling activity (Figure 2D). This indicates that the ECL-2b 'protein plug' in GPR91 may function as a tethered inverse agonist — i.e. a structural component which keeps the unoccupied receptor silent, which may also be the case in the closely related purinergic receptors. It should be noted that although many — and even key — residues of the main ligand binding pocket are conserved among the purinergic receptors and GPR91, the 'previously unnoticed' ArgVI:23, which we find is very important for binding and

activity of both succinate and the novel synthetic agonists, is not conserved in the P2Y1 and in the P2Y12, where this position is occupied by an asparagine and a tyrosine residue, respectively. This may be the major reason why succinate does not work in these other closely related receptors. Although the novel synthetic agonists probably also obtain some of their selectivity through their interaction with the GPR91-unique, ArgVI:23 these larger compounds in addition interact with residues in the extended side-pocket, which also differs between GPR91 and the purinergic receptors.

4.3. GPR91 as a potential drug target

GPR91 appears to be a highly interesting drug target due to its role as a sensor of succinate accumulation, which occurs in multiple conditions as an important part of the cellular response to metabolic stress and hypoxia. The major molecular regulator of succinate concentrations, SDH is an enzyme complex central not only to the TCA cycle but also the electron transport chain (complex II). Thus, when succinate is oxidized to fumarate, FAD is reduced and electrons are channeled to ubiquinone through SDH [48]. Inhibition of SDH activity and the associated accumulation of succinate is observed in response to ischemia [11], hypoxia [49], and hyperglycemia [15], and the accompanying GPR91-induced responses are linked with beneficial tissue adaptation to hypoxia/ischemia such as VEGF production in brain and retina [13,50], cardiac hypertrophy [51], hepatic stellate cell transdifferentiation [4], and renin release [9]. However, when the succinate accumulation and GPR91 stimulation becomes more chronic, as for example in response to hyperglycemia in diabetic patients [15], these effects become harmful. Importantly, GPR91 also plays a central role in the massive infiltration of macrophages that is driving the low grade inflammation associated with obesity [12]. However, although GPR91 in many ways appears to be an attractive new drug target in relation to very difficult indications, such as diabetic retinopathy and nephropathy [15], very little is in fact still known about the basic physiology and pharmacology of this receptor. The structural simplicity of the ligand and the postulated tight binding pocket of GPR91 have probably been discouraging factors for the pharmaceutical exploration of this receptor. The new, highly selective GPR91 ligands, which are devoid of succinate metabolite-like actions, represent great tools to help clarify both the physiological function and the pharmacological potential of GPR91 as here exemplified by the effects on cytokine expression in the alternatively activated (M2) macrophages. Recently, Geubelle and coworkers published a couple of small conformationally constrained succinate analogs cis-epoxysuccinic acid (cESA) and cis-cyclopropane-1,2-dicarboxylic acid (cCPDA) (Figure S5), the latter of which was also an initial hit in our study, as being GPR91 full agonists with potencies similar to succinate itself but devoid of SDH activity [29]. The best of the synthetic compounds identified in the present study, compounds 130 and 131 display higher potency but slightly less efficacy. Importantly, as opposed to cESA and cCPDA, the chemical series of GPR91 agonists presented here offers straight forward medicinal chemistry possibilities for further optimization in respect of efficacy and potency. These ligands could serve not only as the basis for further development of GPR91 agonists with, for example, differential signaling properties, but because many of them are partial agonists, they may also serve as starting points for the development of antagonists, which likely will be the preferred GPR91 drug, although this is still unclear due to the lack of useful pharmacological tools — until now. In 2011, a series of synthetic GPR91 antagonists were published [52]. Some of these antagonists were

orally active and inhibited succinate induced hypertension; however, further development of these have to our knowledge not been reported. Succinate analogs like the ones described here or in a potential antagonistic form will most likely have a relatively low bioavailability. To circumvent this, we have synthesized a pro-drug of compound 130 converting the two carboxylates into esters. Preliminary data using this pro-drug are very promising as high plasma concentrations of compound 130 can be measured after oral administration in mice, indicating that it should be possible to use compounds from this chemical series to study effects of selective GPR91 activation also in the *in vivo* setting after oral administration.

GPR91 is just one out of many receptors through which key metabolites control endocrine and metabolic tissues and immune cell function, for which the physiological in most cases still is poorly understood [1,53]. For some of these receptors, such as HCAR2 (GPR109a), many different types of pharmacological tools are available because the receptor previously has been probed as drug targets for 'the wrong' indications [1]. However, for most of the metabolite receptors such compounds are unfortunately not available. Through computationally based techniques such as those described in the present study it is likely that useful, synthetic non-metabolite ligands can be identified also for the other metabolite receptors and for other interesting GPCRs in general.

AUTHOR CONTRIBUTIONS

T.W.S., T.M.F., and M.T. conceived the project and designed the research. T.M.F. performed molecular modeling, computational chemical analysis and selection of chemical libraries. M.T. performed the experiments. C.M. and S.A.H. provided macrophages and GPR91 expression data in these. E.R.U. designed synthetic routes and supervised synthesis, and E.R.U and M.B. synthesized enantiomerically pure compounds. The manuscript was written by T.W.S., M.T., and T.M.F. with input from all authors.

ACKNOWLEDGEMENTS

CONFLICT OF INTEREST

The authors declare no competing financial interests.

APPENDIX A. SUPPLEMENTARY DATA

Supplementary data related to this article can be found at https://doi.org/10.1016/j.molmet.2017.09.005.

REFERENCES

[1] Husted, A.S., Trauelsen, M., Rudenko, O., Hjorth, S.A., Schwartz, T.W., 2017. GPCR-mediated signaling of metabolites. Cell Metabolism 25:777–796.

[2] He, W., Miao, F.J., Lin, D.C., Schwandner, R.T., Wang, Z., Gao, J., et al., 2004. Citric acid cycle intermediates as ligands for orphan G-protein-coupled receptors. Nature 429:188–193.

[3] de Castro Fonseca, M., Aguiar, C.J., da Rocha Franco, J.A., Gingold, R.N., Leite, M.F., 2016. GPR91: expanding the frontiers of Krebs cycle intermediates. Cell Communication and Signaling 14:3.

[4] Correa, P.R., Kruglov, E.A., Thompson, M., Leite, M.F., Dranoff, J.A., Nathanson, M.H., 2007. Succinate is a paracrine signal for liver damage. Journal of Hepatology 47:262–269.

[5] Li, Y.H., Woo, S.H., Choi, D.H., Cho, E.H., 2015. Succinate causes alpha-SMA production through GPR91 activation in hepatic stellate cells. Biochemical and Biophysical Research Communications 463:853–858.

[6] Kushnir, M.M., Komaromy-Hiller, G., Shushan, B., Urry, F.M., Roberts, W.L., 2001. Analysis of dicarboxylic acids by tandem mass spectrometry. High-throughput quantitative measurement of methylmalonic acid in serum, plasma, and urine. Clinical Chemistry 47:1993–2002.

[7] Sadagopan, N., Li, W., Roberds, S.L., Major, T., Preston, G.M., Yu, Y., et al., 2007. Circulating succinate is elevated in rodent models of hypertension and metabolic disease. American Journal of Hypertension 20:1209–1215.

[8] Wishart, D.S., Jewison, T., Guo, A.C., Wilson, M., Knox, C., Liu, Y., et al., 2013. HMDB 3.0—the human metabolome database in 2013. Nucleic Acids Research 41:D801–D807.

[9] Toma, I., Kang, J.J., Sipos, A., Vargas, S., Bansal, E., Hanner, F., et al., 2008. Succinate receptor GPR91 provides a direct link between high glucose levels and renin release in murine and rabbit kidney. Journal of Clinical Investigation 118:2526–2534.

[10] Cummins, T.D., Holden, C.R., Sansbury, B.E., Gibb, A.A., Shah, J., Zafar, N., et al., 2014. Metabolic remodeling of white adipose tissue in obesity. American Journal of Physiology — Endocrinology And Metabolism 307:E262–E277.

[11] Chouchani, E.T., Pell, V.R., Gaude, E., Aksentijevic, D., Sundier, S.Y., Robb, E.L., et al., 2014. Ischaemic accumulation of succinate controls reperfusion injury through mitochondrial ROS. Nature 515:431–435.

[12] van Diepen, J.A., Robben, J.H., Hooiveld, G.J., Carmone, C., Alsady, M., Boutens, L., et al., 2017. SUCNR1-mediated chemotaxis of macrophages aggravates obesity-induced inflammation and diabetes. Diabetologia 60:1304–1313.

[13] Hu, J., Li, T., Du, X., Wu, Q., Le, Y.Z., 2017. G protein-coupled receptor 91 signaling in diabetic retinopathy and hypoxic retinal diseases. Vision Research.

[14] Sapieha, P., Sirinyan, M., Hamel, D., Zaniolo, K., Joyal, J.S., Cho, J.H., et al., 2008. The succinate receptor GPR91 in neurons has a major role in retinal angiogenesis. Nature Medicine 14:1067–1076.

[15] Peti-Peterdi, J., 2010. High glucose and renin release: the role of succinate and GPR91. Kidney International 78:1214–1217.

[16] Regard, J.B., Sato, I.T., Coughlin, S.R., 2008. Anatomical profiling of G protein-coupled receptor expression. Cell 135:561–571.

[17] McCreath, K.J., Espada, S., Galvez, B.G., Benito, M., de Molina, A., Sepulveda, P., et al., 2015. Targeted disruption of the SUCNR1 metabolic receptor leads to dichotomous effects on obesity. Diabetes 64:1154–1167.

[18] Rubic, T., Lametschwandtner, G., Jost, S., Hinteregger, S., Kund, J., Carballido-Perrig, N., et al., 2008. Triggering the succinate receptor GPR91 on dendritic cells enhances immunity. Nature Immunology 9:1261–1269.

[19] Littlewood-Evans, A., Sarret, S., Apfel, V., Loesle, P., Dawson, J., Zhang, J., et al., 2016. GPR91 senses extracellular succinate released from inflammatory macrophages and exacerbates rheumatoid arthritis. Journal of Experimental Medicine 213:1655–1662.

[20] Letouze, E., Martinelli, C., Loriot, C., Burnichon, N., Abermil, N., Ottolenghi, C., et al., 2013. SDH mutations establish a hypermethylator phenotype in paraganglioma. Cancer Cell 23:739–752.

[21] Selak, M.A., Armour, S.M., MacKenzie, E.D., Boulahbel, H., Watson, D.G., Mansfield, K.D., et al., 2005. Succinate links TCA cycle dysfunction to oncogenesis by inhibiting HIF-alpha prolyl hydroxylase. Cancer Cell 7:77–85.

[22] Due-Hansen, M.E., Pandey, S.K., Christiansen, E., Andersen, R., Hansen, S.V.F., Ulven, T., 2016. A protocol for amide bond formation with electron deficient amines and sterically hindered substrates. Organic and Biomolecular Chemistry 14:430–433.

Original Article

[23] Bruno, N.C., Tudge, M.T., Buchwald, S.L., 2013. Design and preparation of new palladium precatalysts for C-C and C-N cross-coupling reactions. Chemical Science 4:916—920.

[24] Leaver-Fay, A., Tyka, M., Lewis, S.M., Lange, O.F., Thompson, J., Jacak, R., et al., 2011. ROSETTA3: an object-oriented software suite for the simulation and design of macromolecules. Methods in Enzymology 487:545—574.

[25] Bottegoni, G., Kufareva, I., Totrov, M., Abagyan, R., 2009. Four-dimensional docking: a fast and accurate account of discrete receptor flexibility in ligand docking. Journal of Medicinal Chemistry 52:397—406.

[26] O'Boyle, N.M., Banck, M., James, C.A., Morley, C., Vandermeersch, T., Hutchison, G.R., 2011. Open Babel: an open chemical toolbox. Journal of Cheminformatics 3:33.

[27] Pfaffl, M.W., 2001. A new mathematical model for relative quantification in real-time RT-PCR. Nucleic Acids Research 29:e45.

[28] Kostenis, E., 2002. Potentiation of GPCR-signaling via membrane targeting of G protein alpha subunits. Journal of Receptors and Signal Transduction Research 22:267—281.

[29] Geubelle, P., Gilissen, J., Dilly, S., Poma, L., Dupuis, N., Laschet, C., et al., 2017. Identification and pharmacological characterization of succinate receptor agonists. British Journal of Pharmacology 174:796—808.

[30] Zhang, D., Gao, Z.G., Zhang, K., Kiselev, E., Crane, S., Wang, J., et al., 2015. Two disparate ligand-binding sites in the human P2Y1 receptor. Nature 520:317—321.

[31] Irwin, J.J., Sterling, T., Mysinger, M.M., Bolstad, E.S., Coleman, R.G., 2012. ZINC: a free tool to discover chemistry for biology. Journal of Chemical Information and Modeling 52:1757—1768.

[32] Bento, A.P., Gaulton, A., Hersey, A., Bellis, L.J., Chambers, J., Davies, M., et al., 2014. The ChEMBL bioactivity database: an update. Nucleic Acids Research 42:D1083—D1090.

[33] Frimurer, T.M., Ulven, T., Elling, C.E., Gerlach, L.O., Kostenis, E., Hogberg, T., 2005. A physicogenetic method to assign ligand-binding relationships between 7TM receptors. Bioorganic & Medicinal Chemistry Letters 15:3707—3712.

[34] Holst, B., Egerod, K.L., Schild, E., Vickers, S.P., Cheetham, S., Gerlach, L.O., et al., 2007. GPR39 signaling is stimulated by zinc ions but not by obestatin. Endocrinology 148:13—20.

[35] Storjohann, L., Holst, B., Schwartz, T.W., 2008. Molecular mechanism of Zn2+ agonism in the extracellular domain of GPR39. FEBS Lett 582:2583—2588.

[36] Schwartz, T.W., Holst, B., 2007. Allosteric enhancers, allosteric agonists and ago-allosteric modulators: where do they bind and how do they act? Trends in Pharmacological Sciences 28:366—373.

[37] Frimurer, T.M., Mende, F., Graae, A.S., Engelstoft, M.S., Egerod, K.L., Nygaard, R., et al., 2017. Model-based discovery of synthetic agonists for the Zn2+-Sensing G-protein-coupled receptor 39 (GPR39) reveals novel biological functions. Journal of Medicinal Chemistry 60:886—898.

[38] Baell, J., Walters, M.A., 2014. Chemistry: chemical con artists foil drug discovery. Nature 513:481—483.

[39] Carlsson, J., Yoo, L., Gao, Z.-G., Irwin, J.J., Shoichet, B.K., Jacobson, K.A., 2010. Structure-based discovery of A(2A) adenosine receptor ligands. Journal of Medicinal Chemistry 53:3748—3755.

[40] Carlsson, J., Coleman, R.G., Setola, V., Irwin, J.J., Fan, H., Schlessinger, A., et al., 2011. Ligand discovery from a dopamine D3 receptor homology model and crystal structure. Nature Chemical Biology 7:769—778.

[41] Katritch, V., Jaakola, V.P., Lane, J.R., Lin, J., Ijzerman, A.P., Yeager, M., et al., 2010. Structure-based discovery of novel chemotypes for adenosine A(2A) receptor antagonists. Journal of Medicinal Chemistry 53:1799—1809.

[42] Kolb, P., Rosenbaum, D.M., Irwin, J.J., Fung, J.J., Kobilka, B.K., Shoichet, B.K., 2009. Structure-based discovery of beta2-adrenergic receptor ligands. Proceedings of the National Academy of Sciences of the United States of America 106:6843—6848.

[43] Ngo, T., Kufareva, I., Coleman, J., Graham, R.M., Abagyan, R., Smith, N.J., 2016. Identifying ligands at orphan GPCRs: current status using structure-based approaches. British Journal of Pharmacology 173:2934—2951.

[44] Kufareva, I., Katritch, V., Stevens, R.C., Abagyan, R., 2014. Advances in GPCR modeling evaluated by the GPCR Dock 2013 assessment: meeting new challenges. Structure 22:1120—1139.

[45] Manglik, A., Lin, H., Aryal, D.K., McCorvy, J.D., Dengler, D., Corder, G., et al., 2016. Structure-based discovery of opioid analgesics with reduced side effects. Nature 537:185—190.

[46] Lansu, K., Karpiak, J., Liu, J., Huang, X.P., McCorvy, J.D., Kroeze, W.K., et al., 2017. In silico design of novel probes for the atypical opioid receptor MRGPRX2. Nature Chemical Biology 13:529—536.

[47] Schwartz, T.W., 1994. Locating ligand-binding sites in 7TM receptors by protein engineering. Current Opinion in Biotechnology 5:434—444.

[48] Rutter, J., Winge, D.R., Schiffman, J.D., 2010. Succinate dehydrogenase—assembly, regulation and role in human disease. Mitochondrion 10:393—401.

[49] Lukyanova, L.D., Kirova, Y.I., 2015. Mitochondria-controlled signaling mechanisms of brain protection in hypoxia. Frontiers in Neuroscience 9:320.

[50] Hamel, D., Sanchez, M., Duhamel, F., Roy, O., Honore, J.C., Noueihed, B., et al., 2014. G-protein-coupled receptor 91 and succinate are key contributors in neonatal postcerebral hypoxia-ischemia recovery. Arteriosclerosis, Thrombosis, and Vascular Biology 34:285—293.

[51] Aguiar, C.J., Rocha-Franco, J.A., Sousa, P.A., Santos, A.K., Ladeira, M., Rocha-Resende, C., et al., 2014. Succinate causes pathological cardiomyocyte hypertrophy through GPR91 activation. Cell Communication and Signaling 12:78.

[52] Bhuniya, D., Umrani, D., Dave, B., Salunke, D., Kukreja, G., Gundu, J., et al., 2011. Discovery of a potent and selective small molecule hGPR91 antagonist. Bioorganic & Medicinal Chemistry Letters 21:3596—3602.

[53] Tan, J.K., McKenzie, C., Marino, E., Macia, L., Mackay, C.R., 2017. Metabolite-sensing G protein-coupled receptors-facilitators of diet-related immune regulation. Annual Review of Immunology 35:371—402.